

Subadult Virtual Anthropology Database (SVAD) Data Collection Protocol: Epiphyseal Fusion, Diaphyseal Dimensions, Dental Development Stages, Vertebral Neural Canal Dimensions

K.E. Stull^{1,2} and L.K. Corron¹

¹Department of Anthropology, University of Nevada, Reno, United States; ²University of Pretoria, South Africa

*Corresponding author contact information:

Dr. Kyra E. Stull
Department of Anthropology
University of Nevada, Reno
1664 N Virginia St MS 0096
Reno, NV 89557 USA
Phone: 775-784-4834
kstull@unr.edu

This document presents the standardized data collection protocols developed to collect skeletal and dental growth and development indicators on medical images (radiographs and computed tomography scans) and dry skeletal elements. The protocols were developed as part of National Institute of Justice Awards 2015 DN-BX- K009 and 2017 DN-BX-0144 and the National Science Foundation BCS-1551913. The collected derivatives that are discussed within this document comprise the Subadult Virtual Anthropology Database (SVAD). Other protocols associated with the SVAD include segmenting bone surfaces (see the *Isosurface & Surface Generation Protocol in Amira™ protocol* and the *CT scan visualization and measurements protocol in Amira™*). All data was collected in KSCollect, a graphical user interface that saves the data in an R data format (RDS) and preserves the data structure. If one is interested in collecting subadult data using the methodology described herein, then the GUI is available for download and subsequent use at <https://github.com/geanes/KScollect>).

If the derivatives of this protocol are used and the methodology discussed in a presentation or publication, then this document needs to be cited. Additionally, we strongly encourage all research using this data or protocol to be submitted to the Subadult Virtual Anthropology Database Zenodo Community to facilitate sharing and discovery of information (<https://zenodo.org/communities/svad/?page=1&size=20>).

Contents

Epiphyseal Fusion.....	3
Anatomical sites scored and associated staging systems	3
Epiphyseal fusion staging systems	4
<i>Seven-stage scoring system</i>	4
<i>Four-stage scoring system</i>	8
<i>Three-stage scoring system</i>	10
<i>Two-stage scoring system (ossification)</i>	11
Diaphyseal Measurements.....	12
Illustrations of skeletal measurements on dry bones	14
Illustrations of Skeletal Measurements on Virtually Reconstructed Bone Surfaces	19
Dental Development Staging System of Permanent Teeth.....	20
Vertebral Neural Canal (VNC) Diameters	21
Error, Agreement, and Consistency rates (Corron et al., 2021)	22
Consistency of epiphyseal fusion stages scored on dry bone and x-ray images – modality and observer specific	22
Consistency of epiphyseal fusion stages scored on dry bone and x-ray images – anatomical site specific	23
Consistency of epiphyseal fusion stages scored on 2D CT scan and scout images – anatomical site specific	24
Intra- and inter-observer agreement of epiphyseal fusion stages scored on CT scans.....	25
Inter-observer agreement of epiphyseal fusion stages scored on scout images	26
TEM, %TEM, and ICC values for intra- and inter-observer errors of diaphyseal measurements	27
Intra- and inter-observer agreements of dental development stages	28
Intra- and inter-observer agreements of vertebral neural canal diameters	29
References.....	30

Epiphyseal Fusion

Anatomical sites scored and associated staging systems

A seven-stage scoring system was used for the six left long bones and calcaneal tuberosity. A three-stage scoring system was used for the pelvis, specifically the ischiopubic ramus and the ilio-ischiatic acetabular epiphysis. The appearance of ossification centers for the carpals, tarsals, patella, and different centers that comprise the proximal and distal humeral epiphyses were scored with a binary system. Table 1 provides the staging system per bone along with the KSCollect abbreviations.

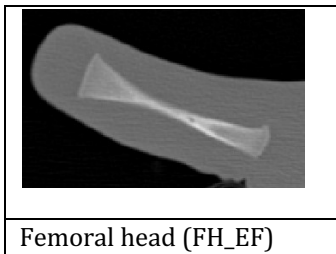
Table 1 – Scoring system per bone with the associated abbreviations.			
Bone	Epiphyses	KSCollect Abbreviation	Scoring System
Humerus	Humeral Head Ossification	HH_Oss	2-stage scoring system
	Humeral Greater Tubercle Ossification	HGT_Oss	
	Humeral Lesser Tubercle Ossification	HLT_Oss	
	Humeral Proximal Epiphyseal Fusion (PE=fused HH, GT and LT). If HPE not fused, score 0 If HPE fused but unfused to diaphysis, score 1	HPE_EF = exists only if HH_Oss + HGT_Oss + HLT_Oss are fused together (stage 0 if absent or present and unfused)	7-stage scoring system
	Capitulum Ossification	HC_Oss	2-stage scoring system
	Trochlea Ossification	HT_Oss	
	Lateral Epicondyle Ossification	HLE_Oss	
	Composite Epiphysis 1 (fusion of capitulum and trochlea) Epiphyseal Fusion	HCE1_EF = H_C + H_T	2-stage scoring system
	Composite Epiphysis 2 (fusion of CE1 and lateral epicondyle) Epiphyseal Fusion	HCE2_EF = HCE1 + HLE	
	Medial Epicondyle Epiphyseal Fusion	HME_EF	2-stage scoring system
	Distal Epiphysis Epiphyseal Fusion (Fusion to the diaphysis)	HDE_EF = HME_EF + HCE_2 Exists only if these elements are present (stage 0 is absent or present and all unfused)	7-stage scoring system
Radius	Proximal Epiphysis Fusion	RPE_EF	7-stage scoring system
	Distal Epiphysis Fusion	RDE_EF	
Ulna	Proximal Epiphysis Fusion	UPE_EF	7-stage scoring system
	Distal Epiphysis Fusion	UDE_EF	
Femur	Femoral Head Epiphyseal Fusion	FH_EF	7-stage scoring system
	Femoral Greater Trochanter Epiphyseal Fusion	FGT_EF	
	Femoral Lesser Trochanter Epiphyseal Fusion	FLT_EF	
	Femoral Distal Epiphysis Epiphyseal Fusion	FDE_EF	
Tibia	Tibial Proximal Epiphysis Epiphyseal Fusion	TPE_EF	7-stage scoring system
	Tibial Distal Epiphysis Epiphyseal Fusion	TDE_EF	
Fibula	Fibular Proximal Epiphysis Epiphyseal Fusion	FBPE_EF	7-stage scoring system
	Fibular Distal Epiphysis Epiphyseal Fusion	FBDE_EF	
Pelvis	Ischio-Pubic Ramus Epiphyseal Fusion	ISPR_EF	3-stage scoring system
	Ilio-Pubic Epiphyseal Fusion	ILPS_EF	
	Ischio-Iliac Epiphyseal Fusion	ILIS_EF	

	Ischio-Pubic Epiphyseal Fusion	ISP_EF	4-stage scoring system
	Iliac Crest Fusion	IC_EF	
Calcaneus	Calcaneal Tuberosity Epiphyseal Fusion	CT_EF	7-stage scoring system
Patella	Patella Ossification	PC_Oss	2-stage scoring system
Carpals	Number of carpals present	CC_Oss	0-8
Tarsals	Number of tarsals present	TC_Oss	0-7

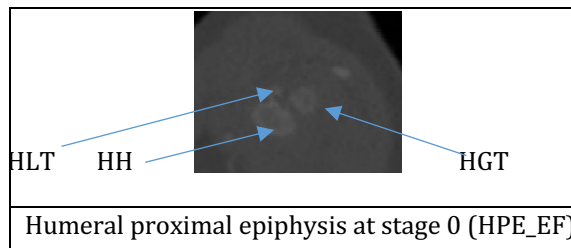
Epiphyseal fusion staging systems

Seven-stage scoring system

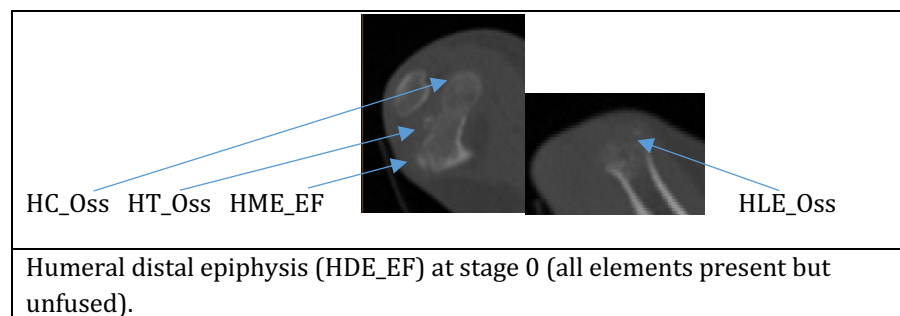
0) “**absent**”: the epiphysis has not ossified (or appeared);



NB: For HPE_EF, stage is 0 if all three elements (Head, Greater Tubercle and Lesser Tubercle) are not fused together. The image below shows all three elements present but not all fused together (HH is only fused to HLT). Hence, assigned stage is 0.

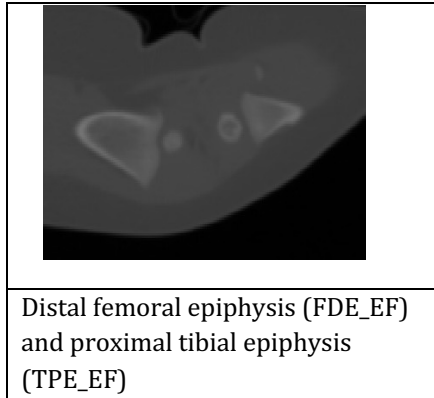


For HDE_EF, stage is 0 if the elements of HCE2_EF (capitulum, trochlea, lateral epicondyle) and HME_EF are not all present. If they are present but unfused, stage is 1.

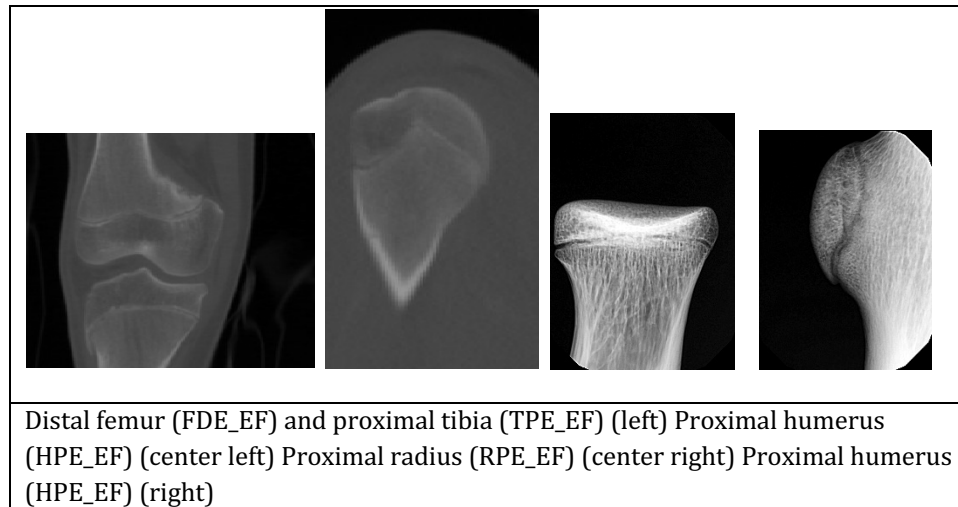


HCE1_EF and HCE2_EF are also scored 0

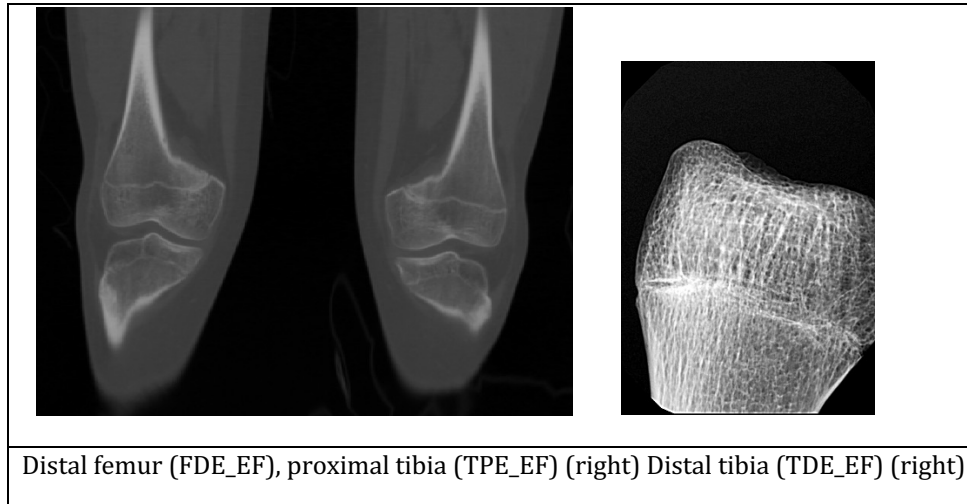
- 1) **“Present”**: the epiphysis has appeared but is characterized by the lack of any bony attachments;



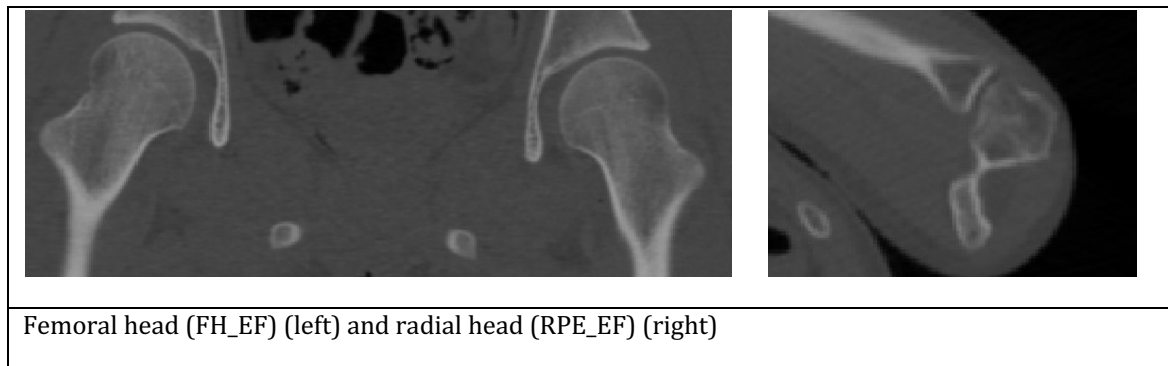
- 2) **“Active Union”** requires metaphyseal trabeculae to cross the epiphyseal growth plate to initiate bone fusion with the epiphysis (with bony bridging equal or slightly less than half the length of the epiphyseal growth plate evident, some gaps maintained throughout). A thick white line or “halo” and some bony bridging can be seen with some parts of the epiphyseal growth plate disconnected from the diaphyseal growth plate;



- 3) **“Advanced Union”** is characterized by bony bridging greater than 75% of the length of the growth plate, with no or minor radiolucent gaps retained throughout;

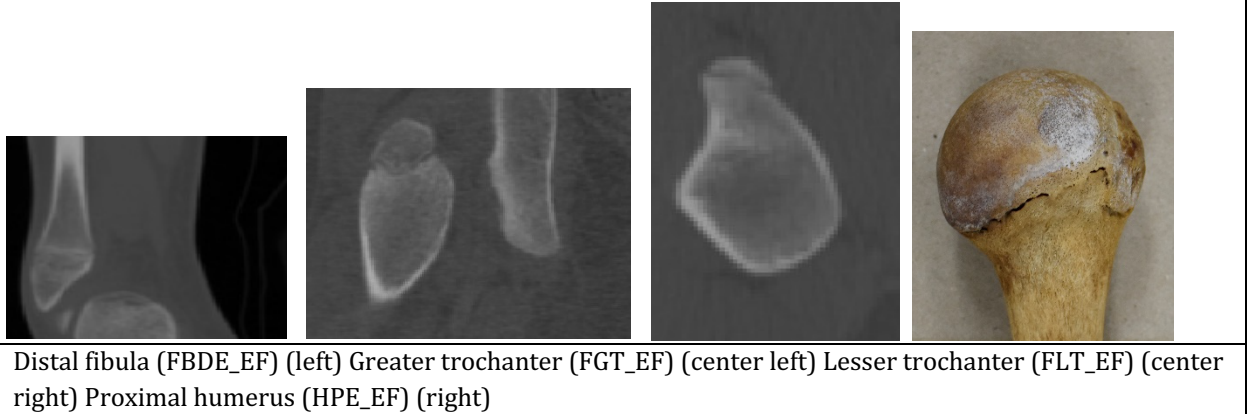


4) **“Complete Union”**, demonstrated by homogenous radiodensity and/or invisible scar.

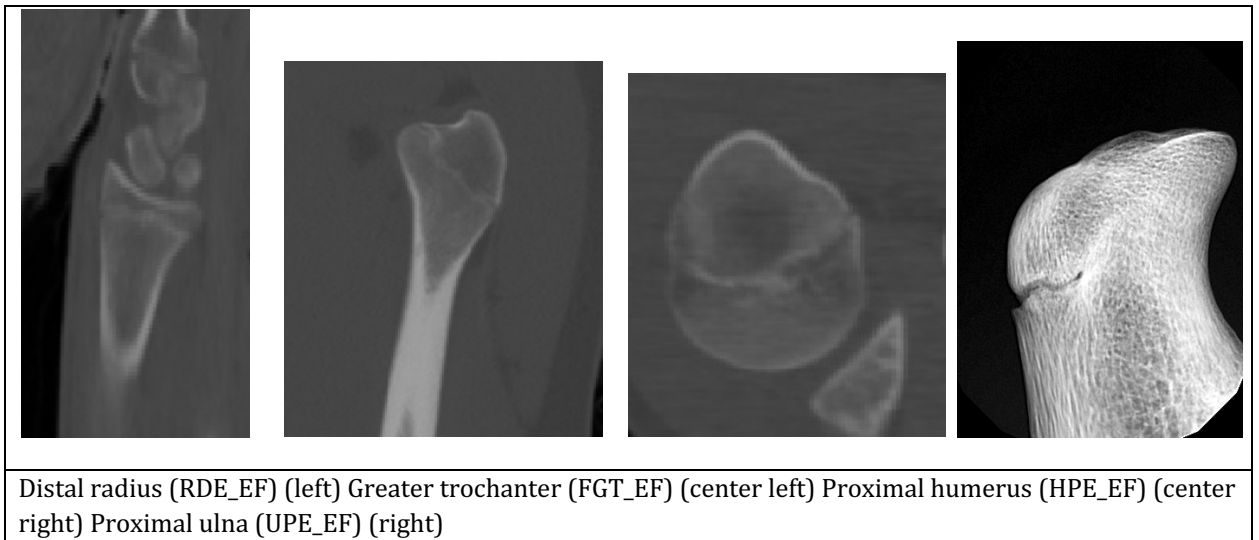


Note: Another two stages, termed **“Early active union”** and **“Active/advanced union,”** can be scored when it is clear that an epiphysis is undergoing fusion (and is therefore in Stage 1 or 2, or 2 or 3 respectively), but a determination of the degree of fusion cannot be reliably made. Stages are transformed numerically into “12” and “23”, respectively.

12) **“Early active union”**: EF is less than 25% and scattered throughout the growth plate



23) **“Active/Advanced union”**: EF is between 50% and 75% and we can't choose between 2 or 3



Four-stage scoring system

0) "absence"



The epiphysis/secondary ossification center is not ossified/absent.

1) "presence but no union"



The epiphysis/secondary ossification center is visible/ossified but unattached to the primary ossification center

2) **“active union”**



The epiphysis/secondary ossification center is partially fused with the primary ossification center

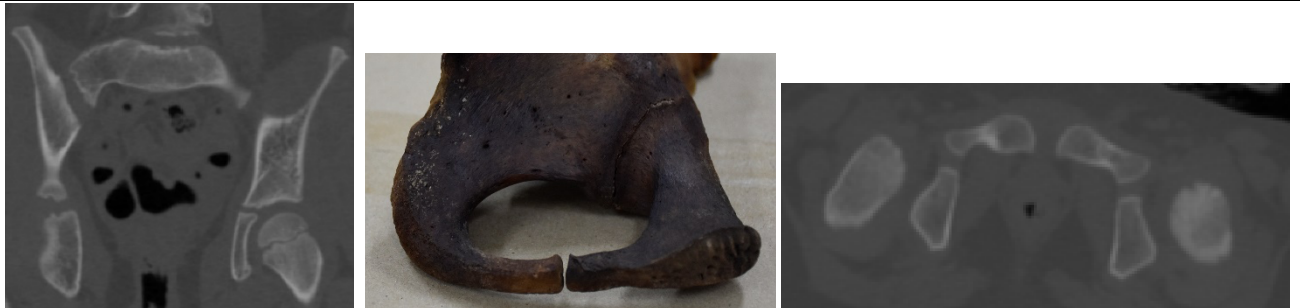
3) **“complete union”**



The epiphysis/secondary ossification center is completely fused with the primary ossification center, the bone is mature.

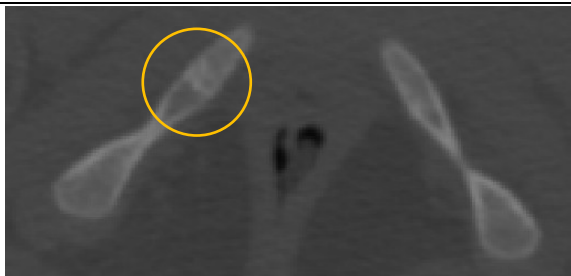
Three-stage scoring system

0) "Unfused"



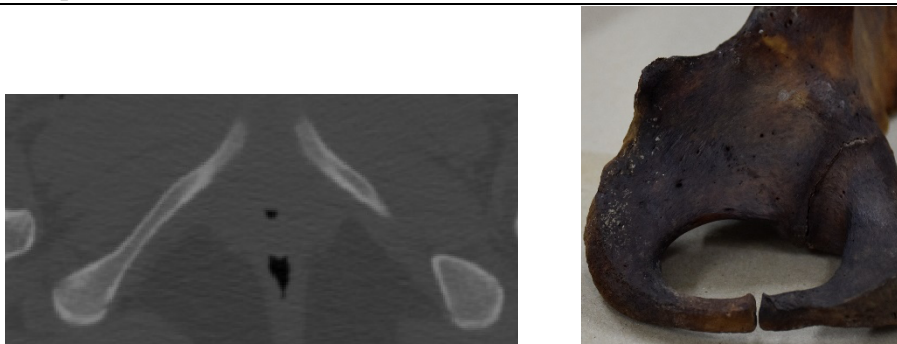
Ilium and ischium (ILIS_EF) (left) Ischium and pubis (ISPR_EF) (middle) Ilium and pubis (left)

1) "Ongoing Fusion"



Ischio-pubic ramus (ISPR_EF) (left)

2) "Complete Fusion"



Ischio-pubic ramus (ISPR_EF) (left) Ilium and ischium (ILIS_EF) (right)

Two-stage scoring system (ossification)

0) **"Absence"**



Capitulum (HC_Oss)

1) **"Presence"**



Capitulum (HC_Oss)

Diaphyseal Measurements

Humerus diaphyseal length (HDL) – The maximum distance between the most proximal edge of the diaphysis to the most distal edge of the diaphysis (modified from Fazekas and Kósa, 1978).

Comment: The most distal portion is generally the medial portion.

Humerus proximal breadth (HPB) – The distance between the most medial and lateral edges of the proximal diaphysis, when the element is viewed in anatomical position.

Comment: This is not a maximum breadth.

Humerus distal breadth (HDB) – The distance between the most medial and lateral points on the distal diaphysis, when the element is viewed in anatomical position (Fazekas and Kósa 1978).

Humerus midshaft breadth (HMSB) – The distance between the most medial and lateral edges at midshaft, perpendicular to the long axis of the bone, when the bone is in anatomical position (Fazekas and Kósa 1978).

Comment: Determine midshaft when obtaining diaphyseal length. Note, this is not a minimum or maximum.

Ulna diaphyseal length (UDL) – The maximum distance between the most proximal edge of the diaphysis to the most distal edge of the diaphysis (Fazekas and Kósa 1978).

Ulna midshaft breadth (UMSB) – The distance between the most medial and lateral edges at midshaft, perpendicular to the long axis of the bone, when the bone is in anatomical position (Fazekas and Kósa 1978).

Comment: Determine midshaft when obtaining diaphyseal length. Note, this is not a minimum or maximum.

Radius diaphyseal length (RDL) – The maximum distance between the most proximal edge of the diaphysis to the most distal edge of the diaphysis (Fazekas and Kósa 1978).

Radius proximal breadth (RPB) – The distance between the most medial and lateral edges of the proximal diaphysis, when the bone is viewed in anatomical position (modified from Urcid, 1992).

Radius distal breadth (RDB) – The distance between the most medial and lateral edges of the distal diaphysis, when the bone is viewed in anatomical position.

Comment: The measurement is obtained from the anterior projections on the distal diaphysis.

Radius midshaft breadth (RMSB) – The distance between the most medial and lateral edges at midshaft, perpendicular to the long axis of the bone, when the bone is in anatomical position (modified from Fazekas and Kósa, 1978).

Comment: Determine midshaft when obtaining diaphyseal length. Note, this is not a minimum or maximum.

Femur diaphyseal length (FDL) – The maximum distance between the most proximal edge of the diaphysis to the most distal edge of the diaphysis (Fazekas and Kósa 1978).

Comment: The most distal point is generally the medial projection on the metaphysis. The expression is slight in infants but becomes more pronounced as age increases.

Femur distal breadth (FDB) – The distance between the most medial and lateral edges of the distal diaphysis, when the bone is viewed in anatomical position (modified from Fazekas and Kósa, 1978).

Femur midshaft breadth (FMSB) – The distance between the most medial and lateral edges at midshaft, perpendicular to the long axis of the bone, when the bone is in anatomical position (Fazekas and Kósa 1978).

Comment: Determine midshaft when obtaining diaphyseal length. Note, this is not a minimum or maximum.

Tibia diaphyseal length (TDL) – The maximum distance between the most proximal edge of the diaphysis to the most distal edge of the diaphysis (Fazekas and Kósa 1978).

Comment: Generally, the most proximal point is medial and the most distal point is lateral.

Tibia proximal breadth (TPB) – The distance between the most medial and lateral edges of the proximal diaphysis, when the bone is viewed in anatomical position (modified from Moore-Jansen et al., 1994).

Tibia distal breadth (TDB) – The distance between the most medial and lateral edges of the distal diaphysis, when the bone is viewed in anatomical position (modified from Moore-Jansen et al., 1994).

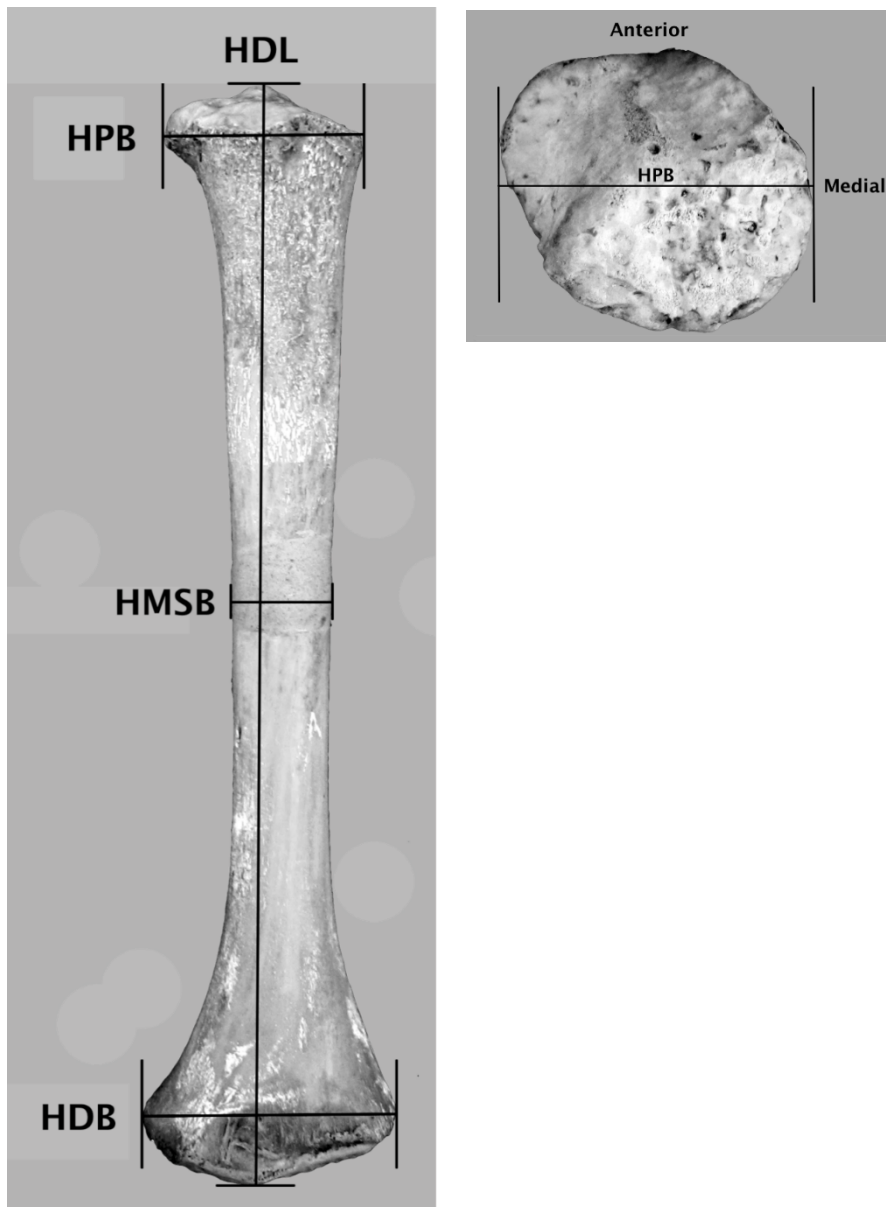
Comment: The lateral edge is the anterior projection of the fibular notch.

Tibia midshaft breadth (TMSB) – The distance between the most medial and lateral edges at midshaft, perpendicular to the long axis of the bone, when the bone is in anatomical position (Fazekas and Kósa 1978).

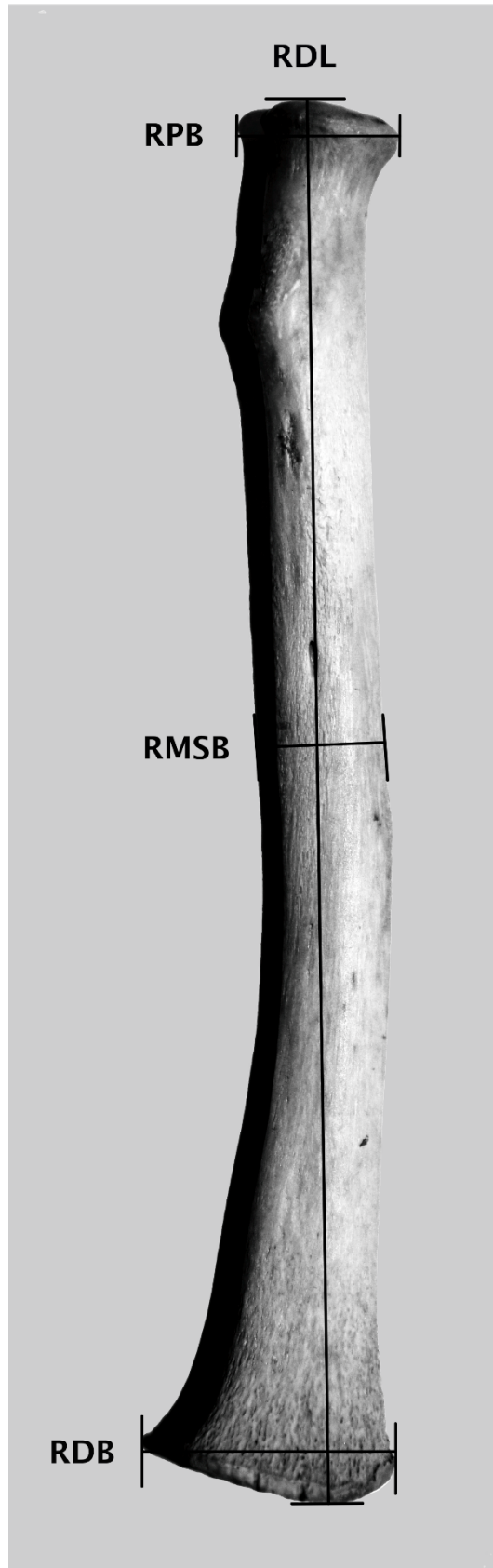
Comment: Determine midshaft when obtaining diaphyseal length.

Fibula diaphyseal length (FBDL) – The maximum distance between the most proximal edge of the diaphysis to the most distal edge of the diaphysis (Fazekas and Kósa 1978).

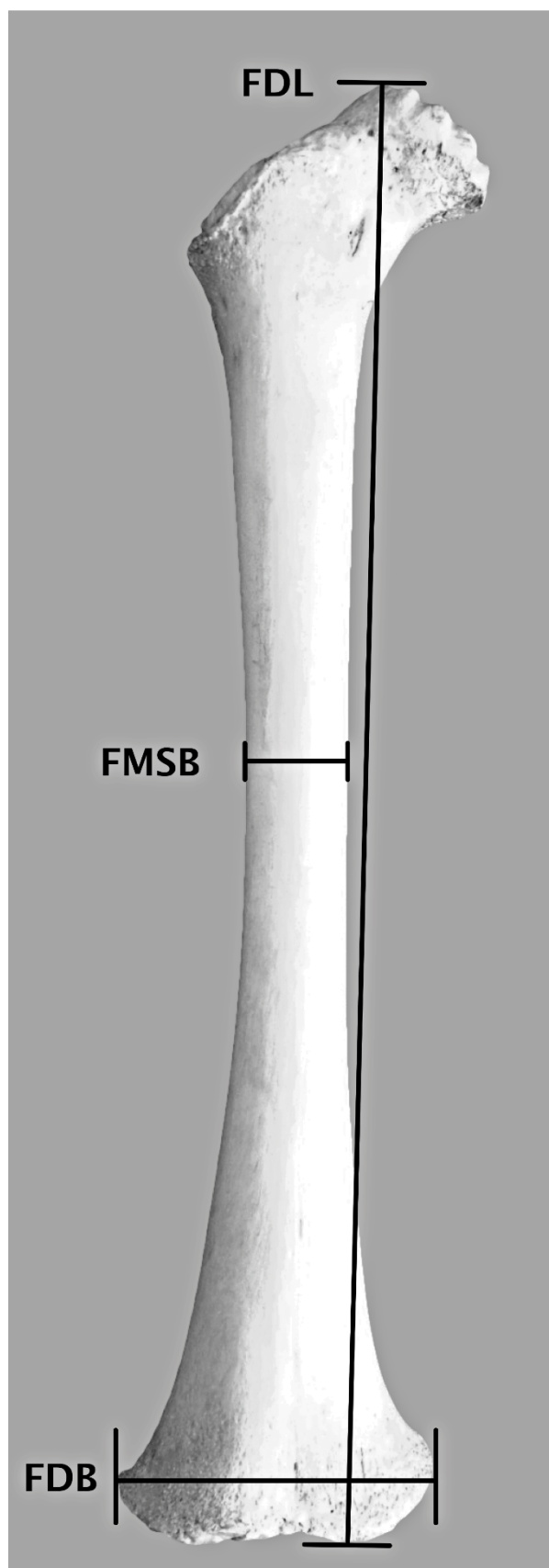
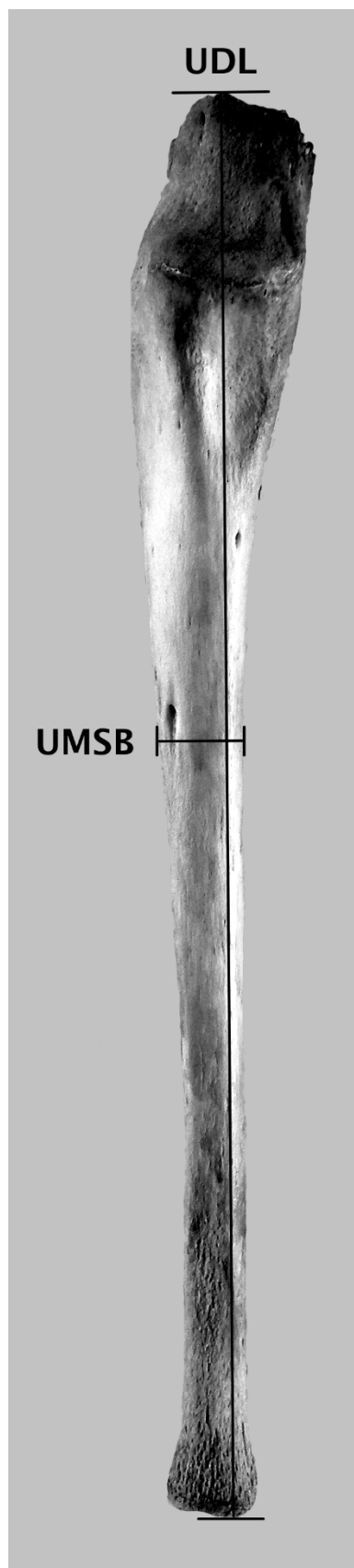
Illustrations of skeletal measurements on dry bones (Stull, L'Abbé, and Ousley 2014)



Superior view of the proximal humerus diaphysis to emphasize the measurement is not a maximum but rather a medial-lateral.

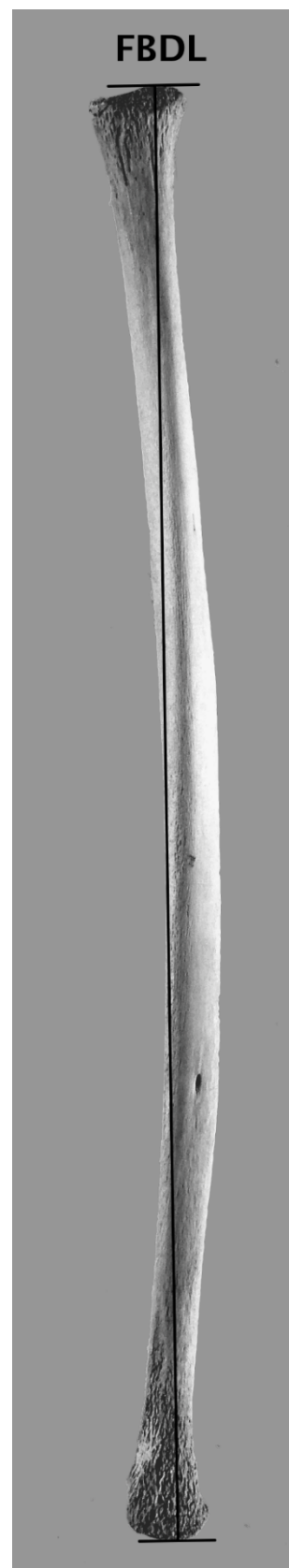
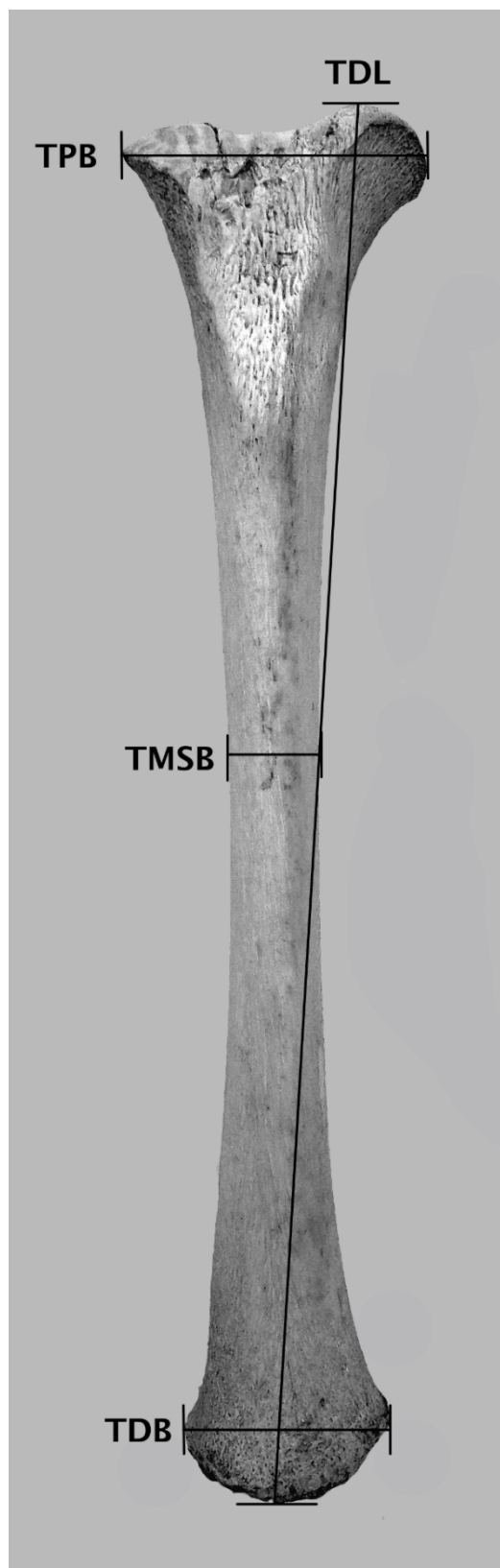


Additional image of the RDB to emphasize the measurement is obtained from the anterior projections on the distal diaphysis.

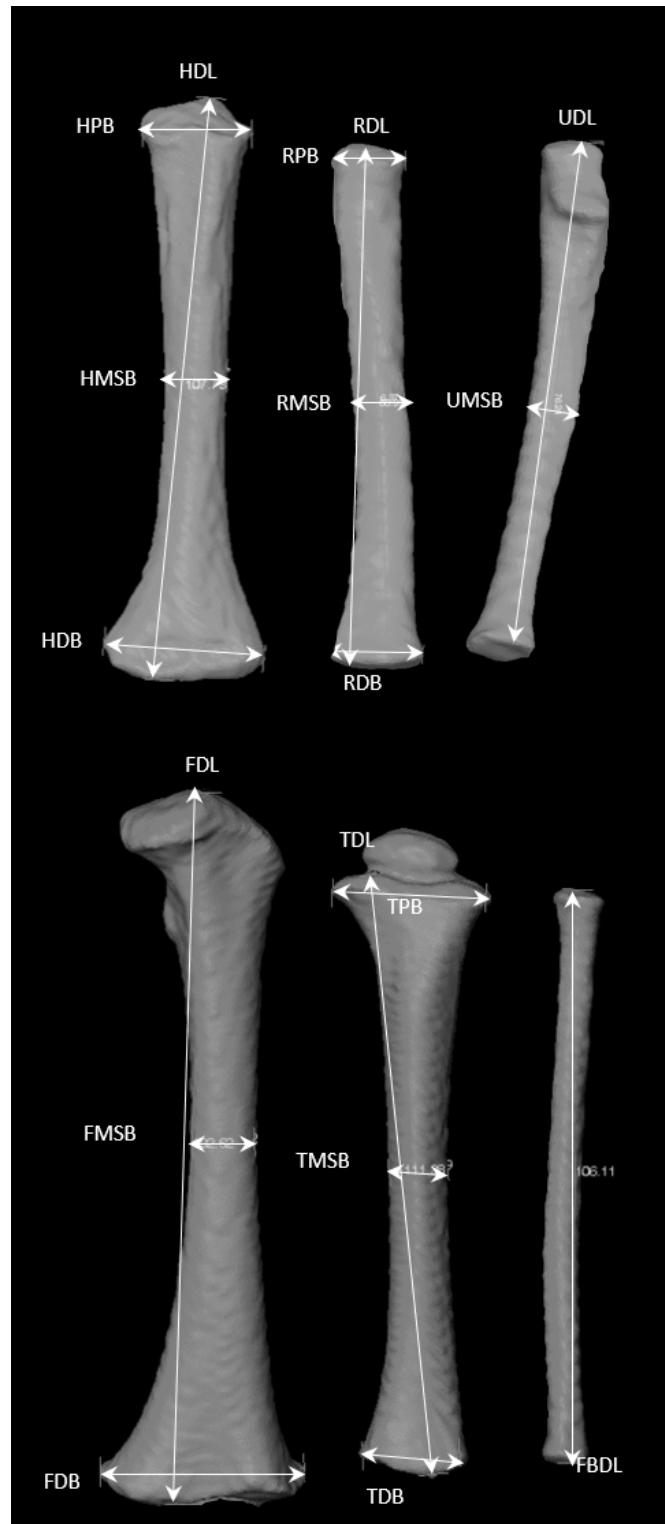




The medial projection of the distal diaphysis of the femur. The expression is slight in younger subadults (left) but is more pronounced in older subadults (right).










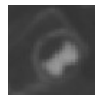





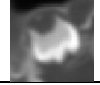







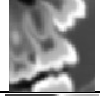




Illustrations of Skeletal Measurements on Virtually Reconstructed Bone Surfaces



Top to bottom and left to right: Humerus, Radius, Ulna, Femur, Tibia, Fibula

Dental Development Staging System of Permanent Teeth

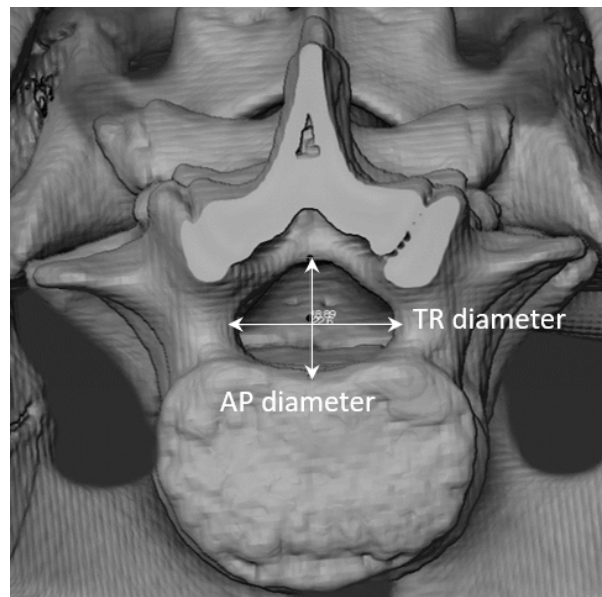
Stage	Monoradicular teeth	Pluriradicular teeth	Description
1			Initial cusp formation
2			Coalescence of cusps
3			Cusp outline complete
4			Crown half completed with dentine formation
5			Crown three quarters completed
6			Crown completed with defined pulp roof
7			Initial root formation with diverge edges
8			Root length less than crown length
9			Root length equals crown length
10			Three quarters of root length developed with diverge ends
11			Root length completed with parallel ends
12			Apex closed (root ends converge) with wide periodontal ligament
13			Apex closed with normal periodontal ligament width

Stages adapted to CT slices from illustrations by AlQahtani, Hector, and Liversidge 2010, which was adapted from Moorrees, Fanning, and Hunt 1963.

Vertebral Neural Canal (VNC) Diameters

Depth (antero-posterior diameter/AP) and width (transverse diameter/TR) of the vertebral neural canal (VNC) measured on the reconstructed surfaces of vertebrae thoracic ten (Th10) to lumbar five (L5) in the superior view following dry bone definitions (Newman and Gowland 2015; Watts 2011; 2013). The 3D measurement tool was used to record measurements to the nearest hundredth of a millimeter.

- **AP diameter** – the distance from the middle of the posterior surface of the vertebral body to the furthest opposite point of the neural canal, anterior to the spinous process
- **TR diameter** – the furthest distance between the medial surfaces of the left and right pedicles once the neural arches have fused at the spinous process



Error, Agreement, and Consistency rates (Corron et al., 2021)

Consistency of epiphyseal fusion stages scored on dry bone and x-ray images – modality and observer specific

Observer	Modalities	Cohen's kappa
Observer 1	Dry bone – x-ray	0.708
Observer 2	Dry bone – x-ray	0.824
Observers 1 and 2	Dry bone (Obs 1) – x-ray (Obs 2)	0.855
	Dry bone (Obs 2) – x-ray (Obs 1)	0.741
	Dry bone (Obs 1 – Obs 2)	0.815
	x-ray (Obs 1 – Obs 2)	0.777

Consistency of epiphyseal fusion stages scored on dry bone and x-ray images – anatomical site specific

Variable	Cohen's kappa value	
	Observer 1	Observer 2
FH_EF	0.804	0.882
FGT_EF	0.868	0.880
FLT_EF	0.714	0.610
FDE_EF	0.787	0.722
TPE_EF	0.702	0.779
TDE_EF	0.934	0.934
FBPE_EF	0.670	1
FBDE_EF	0.931	0.933
HH_Oss	0.643	0.643
HGT_Oss	0.800	0.900
HLT_Oss	0.700	0.900
HPE_EF	0.794	0.664
HC_Oss	0.675	0.483
HT_Oss	1	0.646
HLE_Oss	1	0.821
HCE1_EF	1	0.38
HCE2_EF	1	0.301
HDE_EF	0.652	0.663
HME_EF	0.634	0.758
RPE_EF	0.546	0.591
RDE_EF	0.871	0.801
UPE_EF	0.448	0.727
UDE_EF	0.429	0.724
CT_EF	0.592	0.505
CC_Oss	0.717	0.622
TC_Oss	0.547	0.769
ISPR_EF	0.601	0.733
ILIS_EF	0.667	0.677
PC_Oss	0.667	1
Mean	0.738	0.726

Consistency of epiphyseal fusion stages scored on 2D CT scan and scout images – anatomical site specific

Variable	Cohen's kappa value	
	CT scan – scout (Obs 1)	CT scan – scout (Obs 2)
FH_EF	0.804	0.882
FGT_EF	0.868	0.880
FLT_EF	0.714	0.610
FDE_EF	0.787	0.722
TPE_EF	0.702	0.779
TDE_EF	0.934	0.934
FBPE_EF	0.670	1
FBDE_EF	0.931	0.933
HH_Oss	0.643	0.643
HGT_Oss	0.800	0.900
HLT_Oss	0.700	0.900
HPE_EF	0.794	0.664
HC_Oss	0.675	0.483
HT_Oss	1	0.646
HLE_Oss	1	0.821
HCE1_EF	1	0.380
HCE2_EF	1	0.301
HDE_EF	0.652	0.663
HME_EF	0.634	0.758
RPE_EF	0.546	0.591
RDE_EF	0.871	0.801
UPE_EF	0.448	0.727
UDE_EF	0.429	0.724
CT_EF	0.592	0.505
CC_Oss	0.717	0.622
TC_Oss	0.547	0.769
ISPR_EF	0.601	0.733
ILIS_EF	0.667	0.677
PC_Oss	0.667	1
Mean	0.738	0.726
Bold == kappa values lower than 0.60		

Intra- and inter-observer agreement of epiphyseal fusion stages scored on CT scans

Variable	Cohen's kappa				Kendall's W
	Obs-1-Obs-1	Obs-1-Obs-2	Obs-1-Obs-3	Obs-2-Obs-3	Obs-1-Obs-2-Obs-3
FH_EF	1.000	0.832	0.833	0.916	0.860
FGT_EF	1.000	0.820	0.859	0.868	0.795
FLT_EF	1.000	1	0.781	0.781	0.772
FDE_EF	0.853	0.787	0.643	0.899	0.642
TPE_EF	1.000	1	0.805	0.805	0.693
TDE_EF	0.853	0.915	0.855	0.855	0.834
FBPE_EF	1.000	1	0.937	0.937	0.940
FBDE_EF	1.000	0.835	0.935	0.871	0.887
HH_Oss	1.000	1	1	1	1
HGT_Oss	1.000	0.798	0.8	0.9	0.865
HLT_Oss	0.800	0.900	0.800	0.800	0.866
HPE_EF	0.741	1	0.557	0.557	0.693
HC_Oss	1.000	1	1	1	1
HT_Oss	0.800	0.733	0.737	0.875	0.822
HLE_Oss	0.783	1	0.737	0.737	0.814
HCE1_EF	0.825	0.857	0.545	0.652	0.561
HCE2_EF	0.909	0.733	0.429	0.467	0.501
HDE_EF	0.875	0.747	0.756	0.770	0.593
HME_EF	0.906	1	0.787	0.787	0.735
RPE_EF	1.000	0.729	0.775	0.889	0.749
RDE_EF	1.000	0.918	0.767	0.869	0.814
UPE_EF	1.000	0.856	0.785	0.700	0.643
UDE_EF	1.000	0.890	0.747	0.884	0.786
CT_EF	1.000	0.876	0.879	0.949	0.836
CC_Oss	1.000	0.869	0.920	0.878	0.736
TC_Oss	1.000	0.922	0.853	0.885	0.800
ISPR_EF	0.884	0.875	1	0.925	0.917
ILIS_EF	1.000	1	0.894	0.894	0.886
PC_Oss	1.000	0.989	1	0.898	0.930
Mean	0.939	0.892	0.807	0.836	0.792
Bold == kappa values lower than 0.60					

Inter-observer agreement of epiphyseal fusion stages scored on scout images

Variable	Cohen's kappa
	Scout (Obs-1- Obs-2)
FH_EF	0.799
FGT_EF	0.937
FLT_EF	0.638
FDE_EF	0.815
TPE_EF	0.913
TDE_EF	1.000
FBPE_EF	0.670
FBDE_EF	0.809
HH_Oss	1.000
HGT_Oss	1.000
HLT_Oss	0.794
HPE_EF	0.658
HC_Oss	0.531
HT_Oss	0.545
HLE_Oss	NA*
HCE1_EF	NA*
HCE2_EF	NA*
HDE_EF	0.627
HME_EF	0.433
RPE_EF	0.565
RDE_EF	0.539
UPE_EF	0.545
UDE_EF	0.275
CT_EF	0.808
CC_Oss	0.802
TC_Oss	0.741
ISPR_EF	0.773
ILIS_EF	0.603
PC_Oss	0.717
Mean	0.713
<p>Bold == kappa values lower than 0.60</p> <p><i>*NAs correspond to the absence of scoring from one or both observers for the variable because of insufficient definition on the scout images.</i></p>	

TEM, %TEM, and ICC values for intra- and inter-observer errors of diaphyseal measurements

Variable	Intra-observer error		Inter-observer error								
			Obs 1-Obs 2		Obs 2-Obs 3		Obs 1-Obs 3		ICC Obs 1-Obs 2-Obs 3		
	TEM (mm)	%TEM	TEM (mm)	%TEM	TEM (mm)	%TEM	TEM (mm)	%TEM	Lower	Mean	Upper
FDL	0.202	0.096	0.399	0.229	0.362	0.2334	0.369	0.239	0.999	1	1
FMSB	0.122	0.824	0.069	0.638	0.077	0.658	0.085	0.701	0.967	0.986	1
FDB	0.102	0.209	0.129	0.278	0.312	0.721	0.346	0.799	0.989	0.99	0.996
TDL	0.308	0.171	0.186	0.137	0.184	0.126	0.105	0.072	1	1	1
TPB	0.146	0.373	0.224	0.679	0.351	1.107	0.239	0.749	0.97	0.986	0.995
TMSB	0.426	0.32	0.079	0.748	0.074	0.638	0.147	1.264	0.955	0.98	0.992
TDB	0.125	0.475	0.102	0.451	0.238	1.04	0.266	1.157	0.967	0.985	0.994
FBDL	0.129	0.0735	0.274	0.207	0.331	0.232	0.096	0.067	0.999	1	1
HDL	0.094	0.069	0.148	0.175	0.261	0.232	0.215	0.191	0.998	0.999	1
HPB	0.1784	0.616	0.154	0.622	0.098	0.419	0.143	0.6	0.98	0.991	0.996
HMSB	0.104	0.821	0.0356	0.465	0.041	0.395	0.066	0.637	0.977	0.99	0.996
HDB	0.137	0.396	0.166	0.513	0.128	0.393	0.184	0.566	0.987	0.994	0.997
RDL	0.187	0.154	0.0705	0.098	0.109	0.124	0.091	0.103	0.999	1	1
RPB	0.263	2.259	0.09	0.877	0.086	0.837	0.07	0.675	0.958	0.981	0.992
RMSB	0.101	1.064	0.0354	0.577	0.065	0.862	0.064	0.842	0.928	0.968	0.988
RDB	0.1026	0.582	0.068	0.4	0.723	4.436	0.136	0.818	0.97	0.986	0.994
UDL	0.173	0.128	0.164	0.204	0.129	0.132	0.22	0.223	0.998	0.999	1
UMSB	0.097	1.094	0.0506	0.86	0.0301	0.412	0.063	0.838	0.928	0.968	0.988
Mean	0.161	0.507	0.136	0.453	0.200	0.722	0.161	0.586	0.961	0.989	0.996

TEM: Technical Error of Measurement (mm)

%TEM: Percentage of Technical Error of Measurement

ICC: Inter-Correlation Coefficient

Intra- and inter-observer agreements of dental development stages

Variable	Cohen's kappa				Kendall's W
	Obs-1-Obs-1	Obs-2-Obs-3	Obs-1-Obs-2	Obs-1-Obs-3	Obs-1-Obs-2-Obs-3
max_M1_L	0.816	0.687	0.796	0.835	0.952
max_M1_R	0.816	0.687	0.796	0.835	0.952
max_M2_L	0.753	0.848	0.848	1.000	0.913
max_M2_R	0.753	0.848	0.848	1.000	0.913
max_M3_L	0.767	1.000	1.000	1.000	1.000
max_M3_R	0.793	1.000	1.000	1.000	1.000
max_PM1_L	0.761	0.706	0.741	0.835	0.962
max_PM1_R	0.761	0.842	0.741	0.682	0.929
max_PM2_L	0.815	0.860	0.754	0.800	0.913
max_PM2_R	0.823	0.829	0.754	0.829	0.913
max_C_L	0.781	0.837	0.854	0.788	0.948
max_C_R	0.781	0.791	0.854	0.788	0.960
max_I1_L	0.638	0.770	0.750	0.689	0.919
max_I1_R	0.638	0.770	0.750	0.689	0.919
max_I2_L	0.585	0.814	0.774	0.720	0.907
max_I2_R	0.585	0.870	0.821	0.720	0.919
man_M1_L	0.796	0.797	0.851	0.745	0.962
man_M1_R	0.767	0.797	0.851	0.745	0.962
man_M2_L	0.898	0.873	1.000	0.873	0.929
man_M2_R	0.898	0.873	1.000	0.873	0.929
man_M3_L	0.792	1.000	0.632	0.632	1
man_M3_R	0.792	1.000	0.632	0.632	1
man_PM1_L	0.829	0.777	0.774	0.944	0.982
man_PM1_R	0.880	0.892	0.840	0.811	0.982
man_PM2_L	0.867	0.875	0.715	0.715	0.919
man_PM2_R	0.867	0.875	0.788	0.715	0.919
man_C_L	0.764	0.775	0.721	0.614	0.943
man_C_R	0.696	0.775	0.721	0.614	0.943
man_I1_L	0.627	0.684	0.735	0.650	0.895
man_I1_R	0.627	0.684	0.735	0.650	0.895
man_I2_L	0.635	0.684	0.721	0.650	0.895
man_I2_R	0.635	0.720	0.701	0.650	0.875
Mean	0.757	0.820	0.797	0.773	0.900

Intra- and inter-observer agreements of vertebral neural canal diameters

Variable	Intra-observer error		Inter-observer error	
	TEM (mm)	% TEM	TEM (mm)	% TEM
L5_AP	0.148	0.849	0.358	2.117
L5_TR	0.142	0.613	0.222	0.943
L4_AP	0.172	1.0403	0.213	1.295
L4_TR	0.112	0.5396	0.201	0.949
L3_AP	0.178	1.104	0.246	1.577
L3_TR	0.1587	0.817	0.2	1.02
L2_AP	0.0813	0.509	0.178	1.147
L2_TR	0.0425	0.2245	0.142	0.741
L1_AP	0.131	0.8066	0.169	1.065
L1_TR	0.054	0.29344	0.124	0.672
TH12_AP	0.137	0.8289	0.135	0.841
TH12_TR	0.0724	0.4	0.159	0.872
TH11_AP	0.0853	0.538	0.172	1.095
TH11_TR	0.0384	0.242	0.222	1.359
TH10_AP	0.07077	0.467	0.23	1.555
TH10_TR	0.02355	0.1607	0.118	0.793
Mean	0.102933	0.589565	0.193063	1.127563

References

- AlQahtani, SJ., MP. Hector, and HM. Liversidge. 2010. "Brief Communication: The London Atlas of Human Tooth Development and Eruption" 142: 461–90.
- Corron, LK., M.K. Stock, S.J. Cole, CN. Hulse, HM. Garvin, AR. Klales, and KE. Stull. 2021. "Standardizing Ordinal Subadult Age Indicators: Testing for Observer Agreement and Consistency across Modalities." *Forensic Sci Int* 320: 110687. <https://doi.org/10.1016/j.forsciint.2021.110687>.
- Fazekas, SA, and F Kósa. 1978. *Forensic Fetal Osteology*. Budapest: Akademiai Kiado.
- Moore-Jansen, Peer H, S D Ousley, and Richard L Jantz. 1994. "Data Collection Procedures for Forensic Skeletal Material." 48. Knoxville: Department of Anthropology, The University of Tennessee.
- Moorrees, CFA, EA Fanning, and EE. Hunt. 1963. "Age Variation of Formation Stages for Ten Permanent Teeth." *Journal of Dental Research* 42 (6): 1490–1502.
- Newman, SL., and RL. Gowland. 2015. "Brief Communication: The Use of Non-Adult Vertebral Dimensions as Indicators of Growth Disruption and Non-Specific Health Stress in Skeletal Populations." *American Journal of Physical Anthropology* 158: 155–64.
- Stock, MK., HM. Garvin, LK. Corron, CN. Hulse, LE. Cirillo, AR. Klales, KL. Colman, and KE. Stull. 2020. "The Importance of Processing Procedures and Threshold Values in CT Scan Segmentation of Skeletal Elements: An Example Using the Immature Os Coxa." *Forensic Science International* 309.
- Stull, Kyra E., Ericka N. L'Abbé, and Stephen D. Ousley. 2014. "Using Multivariate Adaptive Regression Splines to Estimate Subadult Age from Diaphyseal Dimensions." *Am. J. Phys. Anthropol.* 154 (3): 376–86. <https://doi.org/10.1002/ajpa.22522>.
- Urcid, Javier. 1992. *Manual for Post-Cranial Measurements*. Smithsonian Institution's National Museum of Natural History.
- Watts, R. 2011. "Non-Specific Indicators of Stress and Their Association with Age at Death in Medieval York: Using Stature and Vertebral Neural Canal Size to Examine the Effects of Stress Occurring during Different Periods of Development." *International Journal of Osteoarchaeology* 21: 568–76.